Motion Estimation Using Point Cluster Method and Kalman Filter

M. Senesh

A. Wolf[1]
e-mail: alonw@technion.ac.il

Biorobotics and Biomechanics Laboratory,
Faculty of Mechanical Engineering,
Technion-Israel Institute of Technology,
Haifa 32000, Israel

The most frequently used method in a three dimensional human gait analysis involves placing markers on the skin of the analyzed segment. This introduces a significant artifact, which strongly influences the bone position and orientation and joint kinematic estimates. In this study, we tested and evaluated the effect of adding a Kalman filter procedure to the previously reported point cluster technique (PCT) in the estimation of a rigid body motion. We demonstrated the procedures by motion analysis of a compound planar pendulum from indirect opto-electronic measurements of markers attached to an elastic appendage that is restrained to slide along the rigid body long axis. The elastic frequency is close to the pendulum frequency, as in the biomechanical problem, where the soft tissue frequency content is similar to the actual movement of the bones. Comparison of the real pendulum angle to that obtained by several estimation procedures—PCT, Kalman filter followed by PCT, and low pass filter followed by PCT—enables evaluation of the accuracy of the procedures. When comparing the maximal amplitude, no effect was noted by adding the Kalman filter; however, a closer look at the signal revealed that the estimated angle based only on the PCT method was very noisy with fluctuation, while the estimated angle based on the Kalman filter followed by the PCT was a smooth signal. It was also noted that the instantaneous frequencies obtained from the estimated angle based on the PCT method is more dispersed than those obtained from the estimated angle based on Kalman filter followed by the PCT method. Addition of a Kalman filter to the PCT method in the estimation procedure of rigid body motion results in a smoother signal that better represents the real motion, with less signal distortion than when using a digital low pass filter. Furthermore, it can be concluded that adding a Kalman filter to the PCT procedure substantially reduces the dispersion of the maximal and minimal instantaneous frequencies. [DOI: 10.1115/1.3116153]

Keywords: rigid body estimation, Kalman filter, point cluster technique

1 Introduction

Reliable data representing the bone motion is essential for the complete understanding of the lower and upper extremity kinematics. Several researchers used markers mounted on the skeletal pins inserted into the bones to measure in vivo kinematics [1–3]. The trajectories of these markers are tracked to estimate the position, velocity, and acceleration of the markers and bones. While this approach generates a valid representation of the motion of the skeletal components of the joint, several characteristics of this method, in particular, its invasive nature, make it inappropriate for everyday clinical measurements.

The most frequently noninvasive method for measuring human locomotion involves placing markers on the skin of the analyzed segment [4]. After markers are placed, opto-electronic systems composed of several high-frequency infrared cameras are used to capture the markers' location in space as a function of time.

Markers attached to the skin are unquestionably safer and easier to use than pin markers. However, estimation of the skeletal motion from the observed markers attached to the skin is significantly affected by the elasticity and nonlinear soft tissue deformation. These deformations result in erroneous calculation of the joint kinematic parameters [4–10] (e.g., joint center and axis of rotation). Furthermore, because of its nature, the artifacts have frequency content similar to the actual bone movement. Therefore, unlike instrument error, it is difficult to reduce it by means of a frequency-based filtering technique [6,11]. The scope and clinical relevance of the in vivo measurement of human motion would be substantially improved if reliable measurements of skeletal movement could be obtained from skin-based marker systems.

Some human motion studies describe three-dimensional in vivo segment motions without taking into consideration the errors associated with nonrigid body movement and the lack of rigorous validation of the methods. Several investigators have described methods that were introduced to reduce errors associated with nonrigid segment movements. These techniques, in general, model the segment as a rigid body, and then apply various estimation algorithms to obtain an optimal estimate of the rigid body motion.

Che'ze et al. [10] proposed a so-called "solidification" procedure to address the marker cluster deformation. The method first identifies the subset of three markers forming the least perturbed triangle throughout the entire motion to define the rigid shape that best fits the time-varying triangle. This triangle is then fitted to each measured triangle using the standard single value decomposition (SVD) algorithm to solve a least-squares positioning problem. This method did not improve the performance obtained using standard SVD algorithm [12].

Lu and O'Connor [13] expanded on the rigid body model approach; rather than seeking optimal rigid body transformation on each segment individually, multiple constrained rigid body transforms are sought, modeling the hip, knee, and ankle as ball and socket joints. The assumption of a ball and socket joint is a limitation of this approach.

Andriacchi et al. [4] approached the segment pose estimation by considering a cluster of markers distributed on a segment, each with assigned weighting factor, which can be varied from sample to sample point cluster technique (PCT). The idea is to adjust the weighting factor of each marker at each step to minimize the

[1]Corresponding author.

Contributed by the Bioengineering Division of ASME for publication in the JOURNAL OF BIOMECHANICAL ENGINEERING. Manuscript received August 20, 2007; final manuscript received September 14, 2008; published online April 13, 2009. Review conducted by Mark Redfern.

 Copyright © 2009 by ASME

Downloaded From: http://biomechanical.asmedigitalcollection.asme.org/ on 01/12/2015 Terms of Use: http://asme.org/terms

changes of the inertia tensor eigenvalues. While these methods have shown initial promise, they remain to be independently verified relative to bone kinematics.

Another type of method is based on a nonlinear state space, using an extended Kalman filter [7,14] and a biomechanical model of the human body. In these works, the distance between the measured markers' trajectories, followed by a Kalman-filter procedure, and the corresponding trajectories in the biomechanical model, is minimized. The biomechanical model used was a simple rigid kinematic chain with an ideal ball in a socket human joint. Therefore, this method does not take into account the mechanical (e.g., range of motion) and pathological (e.g., lost of degree of freedom) characteristics and lacks general validation.

The purpose of this study is to test and evaluate the effect of adding a Kalman-filter procedure to the previously reported PCT method in the estimation of a rigid body motion. Our research hypothesis is that adding a Kalman filter to the PCT method will result in a smoother signal that better represents the real motion. The methods were tested on a compound planar pendulum using indirect opto-electronic measurements of markers attached to an elastic appendage that is restrained to slide along the pendulum. Comparison of a measured rotation angle to that obtained by estimation procedures enables evaluation of the methods' accuracy and the contribution of the Kalman filter to the accuracy of the estimation.

2 Methodology

2.1 PCT. The PCT method [4] is based on a cluster of points uniformly distributed on each segment. Each point is assigned with an arbitrary weighting factor, which can be varied at each time step.

The location of marker i in the global (lab) coordinated system is measured and the center of mass of the points is calculated as a function of the weighting factor. Then, the inertia tensor $I(t)$ for the discrete cluster points is calculated as a function of the weighting factor and of the location of all markers in the global coordinated system, which is located at the center of mass of the points.

The eigenvectors E_j of $I(t)$ were used to form the transformation matrix $R(t)$ as follows:

$$R(t) = (E(t)_1, E(t)_2, E(t)_3) \tag{1}$$

It should be pointed out that the procedure does not always yield a "legal" rotation matrix (Appendix).

The three eigenvectors have the form

$$E(t)_j = \begin{bmatrix} e(t)_{j,x} \\ e(t)_{j,y} \\ e(t)_{j,z} \end{bmatrix}, \quad j = 1,2,3 \tag{2}$$

associated with each of these eigenvectors in an eigenvalue $\lambda(t)_j$, $j=1,2,3$.

The eigenvalues form a basis for an optimization technique since they should remain invariant if the segment moves as a rigid body. If nonrigid body movement occurs, the eigenvalues will change their value during movement. An algorithm was developed to minimize the eigenvalue changes by redistributing the weight factor at each time step. At each time step, the eigenvalues and the sum of squares of the three eigenvalues (eigenvalues' norm) were calculated as a function of the mass distribution:

$$\Lambda_i = \sqrt{(\lambda_i)_1^2 + (\lambda_i)_2^2 + (\lambda_i)_3^2} \tag{3}$$

The difference between Λ_0 (the eigenvalues' norm at rest position) and Λ_s (the eigenvalues' norm at t_s) could be calculated in terms of n cluster points weighting factor for each time step. This difference was defined as a function

$$F = (\Lambda_s - \Lambda_0)^2 \tag{4}$$

Minimization of F was solved numerically using unconstrained nonlinear optimization operator in MATLAB™. The mass distribution was defined in terms of a single distribution parameter and calculated such that the point with the largest displacement from the rest position, in the local (cluster) coordinate system, was assigned the lowest weighting factor.

At each time step, the rotation matrix (R_i^G), which describes the rotation from the cluster system (local system-i) to the global (lab-G) system, was calculated. To calculate the segment's screw angle in a local coordinate system, at each time step, the rotation matrix (R_i^G) was multiplied by the rotation matrix that describes the rotation from the global system to the local system in the rest position (R_G^0). The latter is equal to $(R_0^G)^T$, which was calculated in the minimization algorithm.

2.2 Kalman Approach to Kinematic Estimation. The Kalman filter is one of the most useful tools available today for estimating the state of a dynamical system in the presence of noise [15]. In the Kalman-filter theory, state variables are collected into a state vector $x(t)$ and undergo dynamic changes through the state function $s(x(t))$. For the Kalman filter to provide good working results, the state function of each variable should represent the true dynamics as accurately as possible.

Avoiding a specific model for the dynamics of the motion, the more general formulation for the state function is the approach used in the field of numerical differentiation [7,14,16]. In this approach, a generic variable $x_k \in x$ can be associated with a Taylor series expansion as

$$\begin{bmatrix} x_k(t+1) \\ x_k^{(1)}(t+1) \\ x_k^{(2)}(t+1) \\ \cdot \\ \cdot \\ \cdot \\ \cdot \\ x_k^{(N)}(t+1) \end{bmatrix} = \begin{bmatrix} 1 & t_s & t_s^2/2! & . & . & . & . & t_s^N/N! \\ 0 & 1 & t_s & t_s^2/2! & . & . & . & t_s^{N-1}/N-1! \\ 0 & 0 & 1 & t_s & t_s^2/2! & . & . & . \\ . & . & . & . & . & . & . & . \\ . & . & . & . & . & . & . & . \\ . & . & . & . & . & . & . & . \\ . & . & . & . & . & . & . & . \\ 0 & . & . & . & . & . & . & 1 \end{bmatrix} \times \begin{bmatrix} x_k(t) \\ x_k^{(1)}(t) \\ x_k^{(2)}(t) \\ . \\ . \\ . \\ . \\ x_k^{(N)}(t) \end{bmatrix} + \begin{bmatrix} n_{k,0}(t) \\ n_{k,1}(t) \\ n_{k,2}(t) \\ . \\ . \\ . \\ . \\ n_{k,N}(t) \end{bmatrix} \tag{5}$$

where $x_k^{(d)}$, t_s, and N are the dth derivatives of the variable, time sampling interval, and series expansion order, respectively. In the proposed study N was taken as $N=2$.

The noise in the model is the Taylor remainder (higher-order derivatives):

$$Q_k(i,j) = \frac{t_s^{2N+3-i-j}}{(N+1-i)\,!\,(N+1-j)\,!\,(2N+3-i-j)}\sigma_k^2 \tag{6}$$

The value σ_k^2 was set up according to the frequency content of the signal and the sampling frequency [16]

$$\sigma_k^2 = \frac{((M\bar{\omega}_k^{N+2}e^{\bar{\omega}_k t_s}/4\pi)t_s)^2}{3t_s} \tag{7}$$

where $\bar{\omega}_k$ and M are calculated from the measurement spectrum (harmonic analysis [17]) and are defined as the signal cutoff frequency and upper bound, respectively.

Downloaded From: http://biomechanical.asmedigitalcollection.asme.org/ on 01/12/2015 Terms of Use: http://asme.org/terms

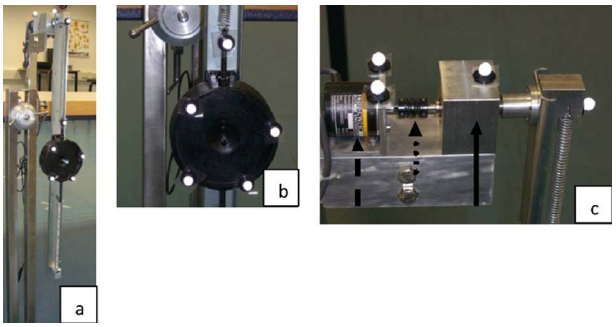

Fig. 1 Experiment setup: (*a*) system setup, (*b*) sliding mass, (*c*) static part, and pendulum hinge

3 Experimental Analysis

3.1 Experiment Setup. The experimental system is composed of a planar pendulum ($M=0.922$ kg) on which an elastic appendage ($m=2.05$ kg) is restrained to slide along (Figs. 1(*a*) and 1(*b*)). The pendulum is mounted on a fixed base via a shaft and a bearing (Fig. 1(*c*), solid line arrow). The shaft is free to rotate and is connected to an encoder (Fig. 1(*c*), dashed line arrow) via a coupler (Fig. 1(*c*), dotted line arrow). Four markers (reflectors) were attached to the static (rigid) part of the pendulum (Fig. 1(*c*)) and five markers were attached to the appendage (Fig. 1(*b*)).

The spring constant is 187.5 N/m (obtained from dynamic analysis of the pendulum motion).

The system's total moment of inertia, estimated from the free vibration of the planar pendulum (where the springs were not connected), is $I_{\text{total}}=0.4278$(kg m).

Plotting the frequency backbone for both the pendulum angle and the slider vibration (Figs. 2(*a*) and 2(*b*)) reveals that the elastic frequency is close to the pendulum frequency, as in the biomechanical problem, where the soft tissue frequency content is similar to the actual movement of the bones. We note that the frequency backbone is obtained by plotting the instantaneous maximal (minimal) amplitudes (Amax/min) versus their corresponding maximal (minimal) frequencies (Fmax/min), where the last are calculated as the harmonic mean of the three opposite consecutive instantaneous periods:

$$F = (T_{i-1}^{-1} + T_i^{-1} + T_{i+1}^{-1})/3 \tag{8}$$

During experiments, the pendulum was oscillating freely about the fixed base while the position of the markers was measured using the vicon motion capture system ($M \times 13$) [18]. Four cameras were used and the pendulum was positioned in the center of the view of each camera. The reported capture system error is 0.1 pixel, which is equivalent to 0.1–0.2 mm (in 3D) [18].

3.2 Experiment Results. In this section, we present the result of the angle calculation compared with the real angle. All data

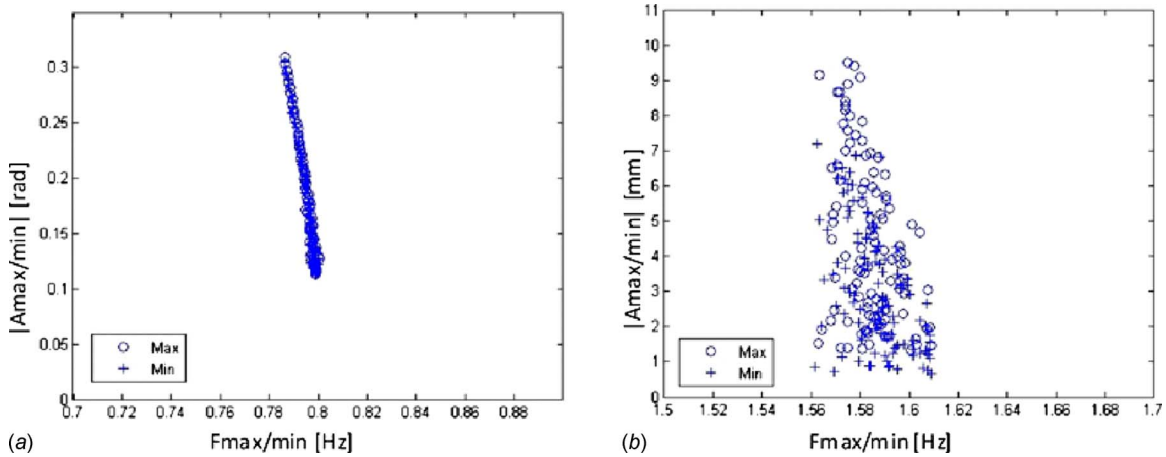

Fig. 2 Frequency backbones: (*a*) pendulum and (*b*) slider mass

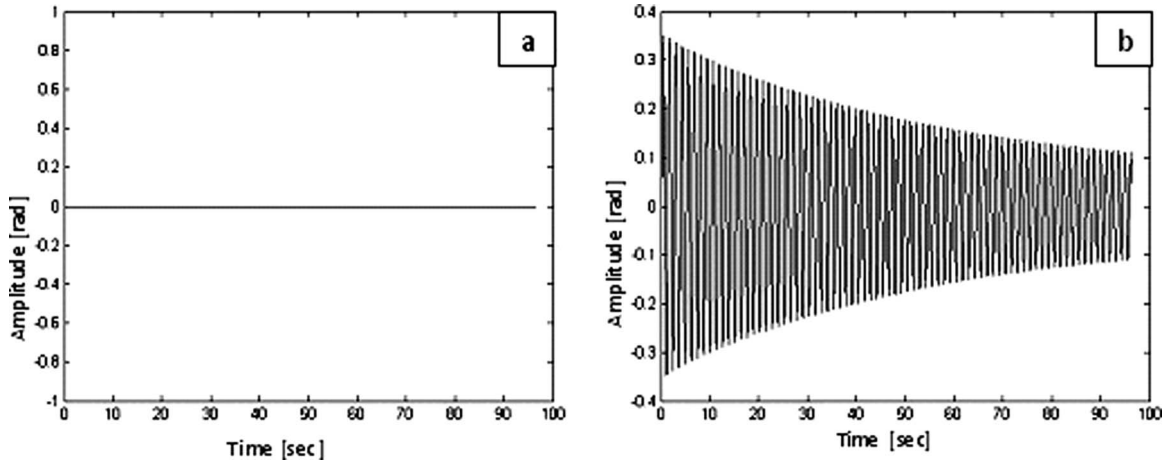

Fig. 3 Real angle: (*a*) static part of the pendulum and (*b*) pendulum hinge

Downloaded From: http://biomechanical.asmedigitalcollection.asme.org/ on 01/12/2015 Terms of Use: http://asme.org/terms

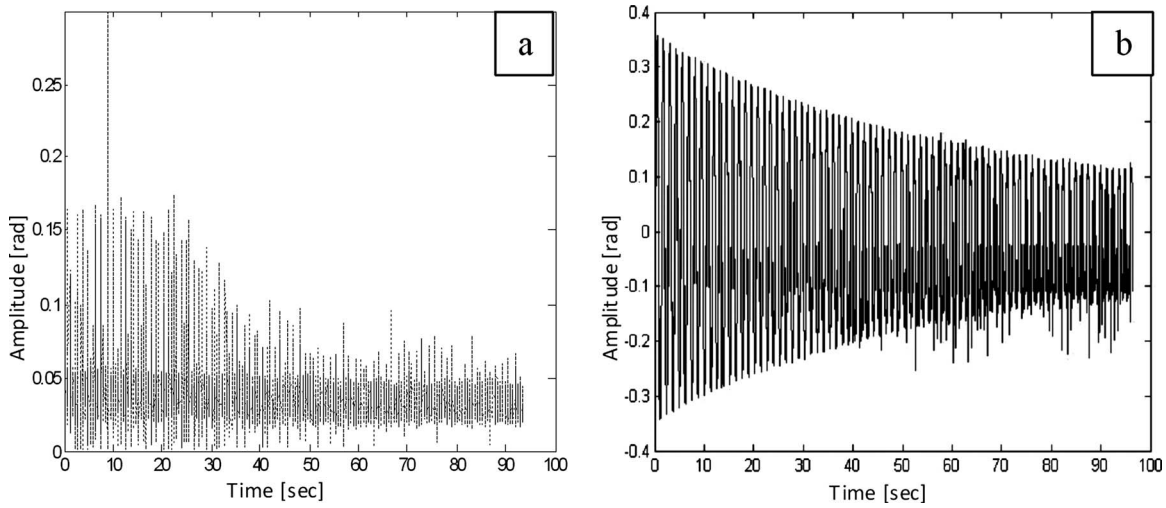

Fig. 4 PCT estimated angle: (*a*) static part of the pendulum and (*b*) pendulum hinge

analysis was done using MATLAB™ 7.2.

The cutoff frequency of $\omega=13$ Hz was evaluated using harmonic analysis [17]. However, in order to get enough noise reduction and less signal distortion, the cutoff frequency was set to $\bar{\omega}_k=20$ Hz. The signal upper bound was also set based on the harmonic analysis to $M=80$ dB.

Figures 3–5 describe the real angles, the PCT estimation angles, and the Kalman filter followed by the PCT estimation angles—of both the static part and pendulum hinge.

Note that for both the static parts of the pendulum and the pendulum hinge, the estimation based on the Kalman filter followed by the PCT yields a less noisy signal compared with the estimation based only on the PCT method.

3.3 Accuracy of the Estimated Response. Several parameters were evaluated in order to compare the accuracy of the two presented methods. The first comparison is between the calculated maximal angular amplitudes (Fig. 6).

The maximal angular amplitudes were estimated as the maximal point of applied cubic spline interpolation on the measured/estimated signal in the apex areas.

A relative error between the maximal angular amplitudes was defined as

$$E_{\%} = ||\theta_m| - |\theta_e||/|\theta_m| \times 100\% \tag{9}$$

where θ_m and θ_e are the measured and estimated maximal angular amplitudes, respectively.

Figure 7 shows that in both methods there is a variant error with a maximal value of $\sim 4\%$.

When comparing the maximal amplitude (Figs. 6 and 7), one can conclude that no significant effect is noted by adding the Kalman filter; however, a closer look at the signal (Fig. 8) reveals that the estimated angle based only on the PCT method is very noisy with fluctuation, and the estimated angle based on the Kalman filter followed by the PCT is a smooth signal.

The second comparison is between the instantaneous maximal (minimal) frequencies (Eq. (8)).

Note that the instantaneous frequencies obtained from the estimated angle based on the PCT method are more dispersed than those obtained from the estimated angle based on the Kalman filter followed by the PCT method (Fig. 9).

The dispersion of the data was estimated as

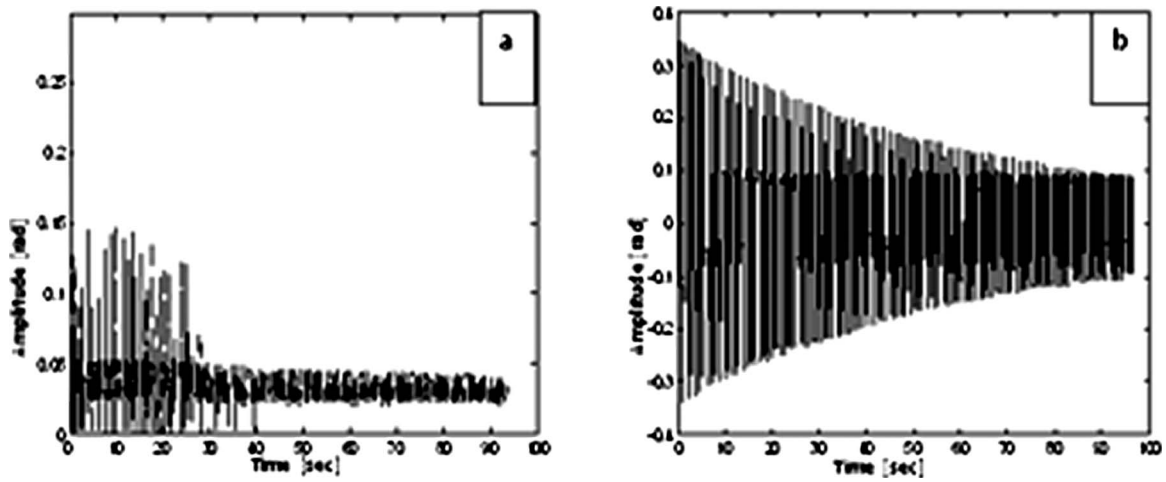

Fig. 5 Kalman filter followed by PCT estimated angle: (*a*) static part of the pendulum and (*b*) pendulum

Downloaded From: http://biomechanical.asmedigitalcollection.asme.org/ on 01/12/2015 Terms of Use: http://asme.org/terms

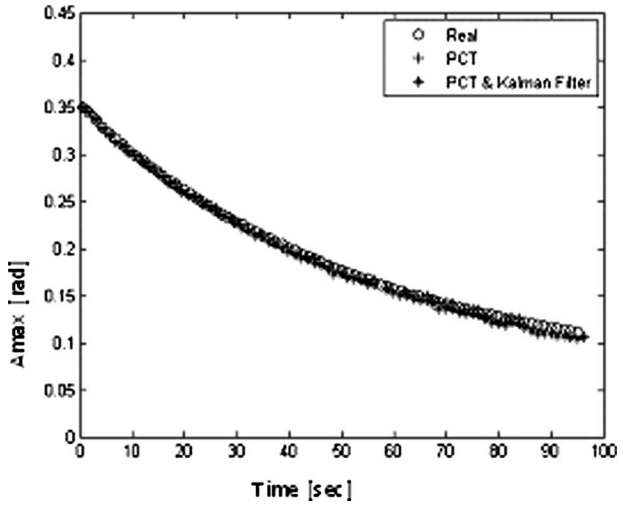

Fig. 6 Maximal angular amplitudes: (+) real angle, (○) PCT estimated angle, and (*) Kalman filter followed by PCT estimated angle

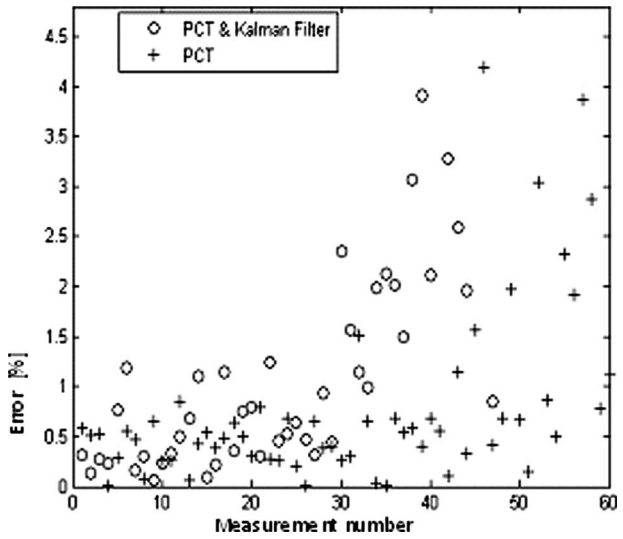

Fig. 7 Relative error between the real and estimated angle: (○) Kalman filter followed by PCT estimated angle and (+) PCT estimated angle

$$s_i = \sqrt{\sum_{i=1}^{n} (F_i - \hat{F}_i)^2/(n-2)} \tag{10}$$

where F_i and $\hat{F}_i$ are the maximal/minimal instantaneous frequencies obtained from the estimated and real angles, respectively, and n is the number of measurements.

A statistic test (F test) has been conducted to determine if the difference in the dispersion is statistically significant.

The F statistics for the maximal and minimal instantaneous frequencies are 19.73 and 18.34, respectively. Both results are much greater than the appropriate F critical ($F_{\text{critical}}=2.62$) for 99% confidence interval.

Therefore, it can be concluded that adding a Kalman filter to the PCT procedure substantially reduces the dispersion of the maximal and minimal instantaneous frequencies.

The results were also compared with an estimated angle using a standard digital low pass filter (Butterworth), which was reported to be used in biomechanics data analysis [17], followed by the PCT algorithm. The low pass filter parameters are a function of a cutoff frequency, which was evaluated as previously described. The estimated angles are presented in Fig. 10.

The relative error between the maximal angular amplitudes as defined in Eq. (9) was also calculated for this procedure, and a two-sided pair t-test was conducted between the errors of the estimated angle based on the Kalman filter followed by the PCT and the errors of the estimated angle based on the low pass filter followed by the PCT. The test P value was 0.0166, which is statistically significant ($P<0.05$). Therefore, it can be concluded that the two relative errors have different mean values. The statistical parameter d was defined as $d=E_{\text{Kalman}}-E_{\text{low pass}}$ and the calculated t parameter was -2.451, which is much smaller than the lower 95% confidence boundary for this case (-0.79077), meaning the mean relative error of the estimated angle based on the Kalman filter followed by the PCT is significantly smaller than the mean relative error of the estimated angle based on the low pass filter followed by the PCT.

Note that when comparing the instantaneous frequency, there was no difference between the two methods.

4 Discussion and Closing Remarks

In this study, we tested and evaluated the effect of adding a Kalman-filter procedure to the previously reported PCT for the estimation of a rigid body motion. The analysis was carried out on an actual mechanical system and not by computer simulation only. The measurements were obtained using the vicon motion system, which is used in human gait analysis.

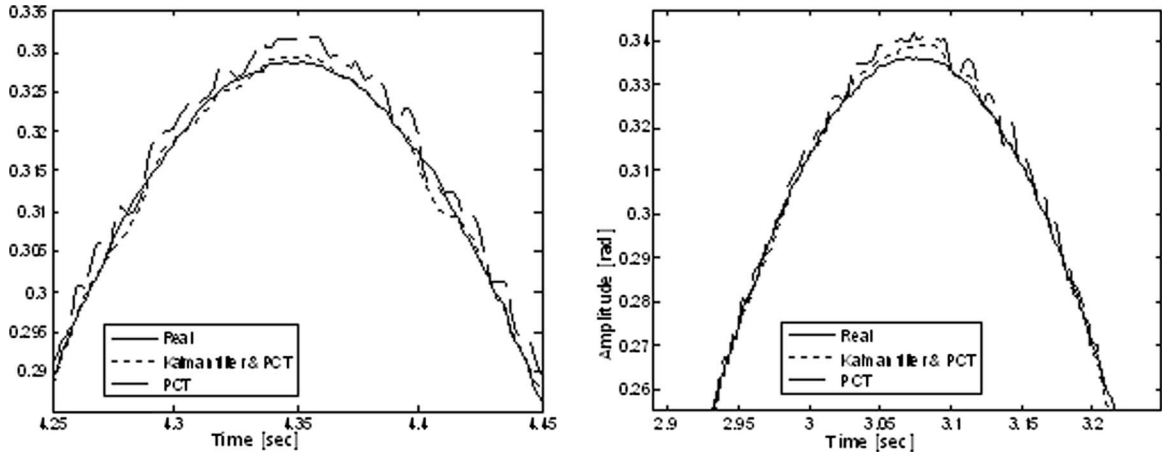

Fig. 8 Closer look at the signals: (−) real angle, (…) PCT estimated angle, and (--) Kalman filter followed by PCT estimated angle

Downloaded From: http://biomechanical.asmedigitalcollection.asme.org/ on 01/12/2015 Terms of Use: http://asme.org/terms

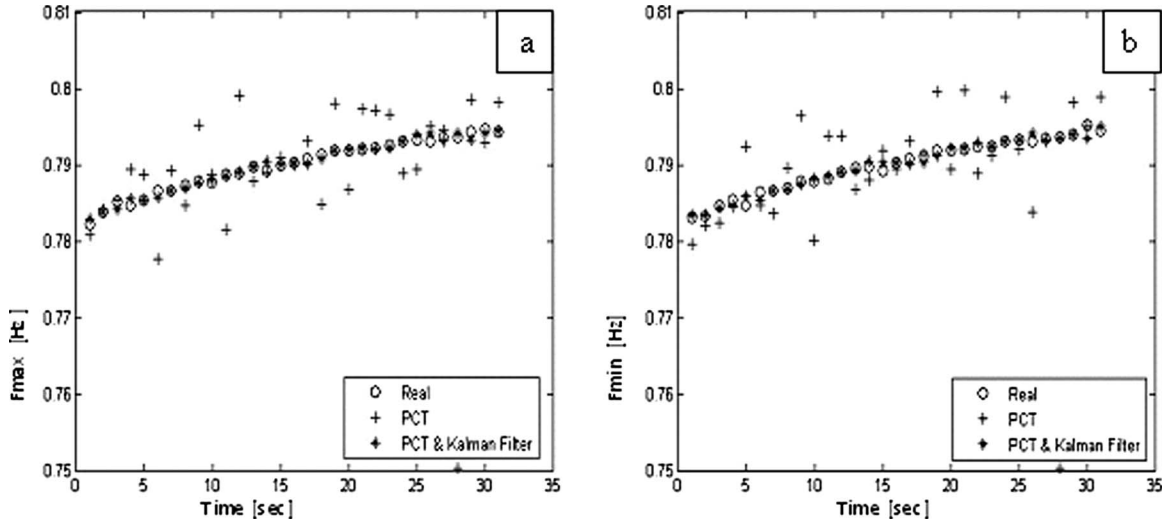

Fig. 9 Instantaneous frequency: (*a*) instantaneous maximal frequency, (*b*) instantaneous minimal frequency. (○) real angle, (+) PCT estimated angle, and (*) Kalman filter followed by PCT estimated angle

The methods were tested on a compound planar pendulum using indirect opto-electronic measurements of markers attached to an elastic appendage that is restrained to slide along the pendulum. The elastic frequency (of the elastic appendage) is closer to the pendulum frequency, as in the biomechanical problem, where the soft tissue frequency content is similar to the actual movement of the bones.

In this simple dynamics system, the rigid rod (pendulum) represents the bone, and the soft tissue is represented by the combination of the two springs and slider mass (Fig. 11).

The idea behind this dynamics system is the description of a soft tissue as a complex set of masses connected with springs. However, we chose to validate the procedure on the simplest system composed of one mass and two springs.

Although this system does not completely simulate the mechanical properties of the human body, we used it since it allows to examine the effectiveness and accuracy of the proposed methods with respect to the true measurement of the rigid body motion, i.e., the pendulum motion. In actual human trials, this comparison cannot be carried out without the use of an invasive method (or high exposure to radiation) to extract real bone motion.

Comparing the maximal amplitude revealed no effect as a result of adding the Kalman filter. However, a closer look at the signal revealed that the estimated angle based on only the PCT method was very noisy with fluctuation, while the estimated angle based on the Kalman filter followed by the PCT was a smooth signal.

It should also be noted that in both the real angle and the estimated angle based on the Kalman filter followed by the PCT method, the cubic spline interpolation followed the actual signal; however, for the estimated angle based on the PCT method only, the interpolation was actually a smooth signal.

Furthermore, it can be concluded that adding a Kalman filter to the PCT procedure substantially reduces the dispersion of the maximal and minimal instantaneous frequencies. The maximal and minimal instantaneous frequencies are indices for the signal phase; therefore, the angle estimation using the PCT leads to a time shift and signal phase inconsistency.

The results of the estimated angle based on a digital low pass filter followed by the PCT method and the estimated angle based on a Kalman filter followed by the PCT method were compared. The relative error of the maximal amplitude in the Kalman filter followed by the PCT method was smaller than that in the low pass filter followed by the PCT method. This means that less signal distortion occurs when using a Kalman filter over a digital low pass filter.

Future research will incorporate controlled human motion ex-

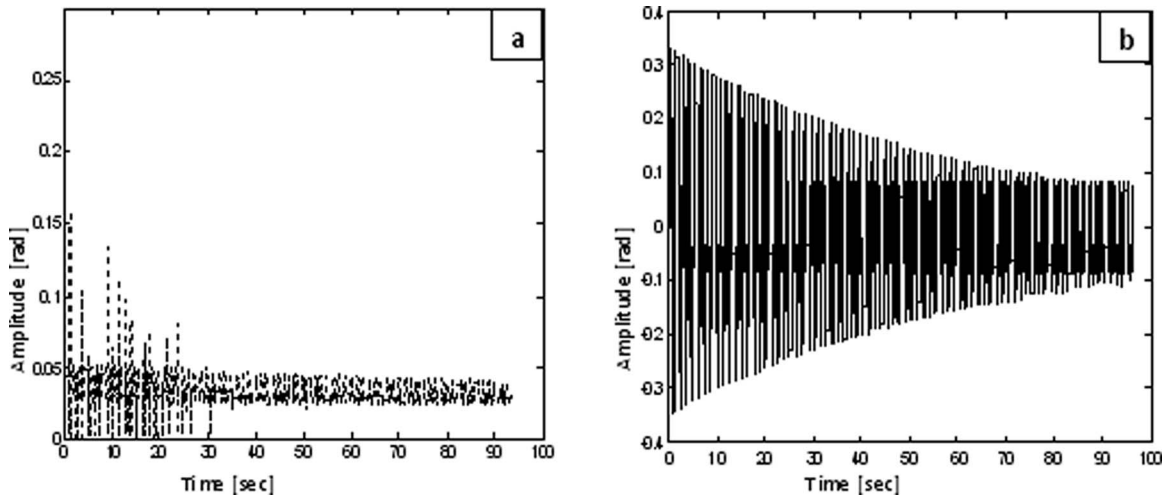

Fig. 10 Low pass filter followed by PCT estimated angle: (*a*) static part of the pendulum and (*b*) pendulum

Downloaded From: http://biomechanical.asmedigitalcollection.asme.org/ on 01/12/2015 Terms of Use: http://asme.org/terms

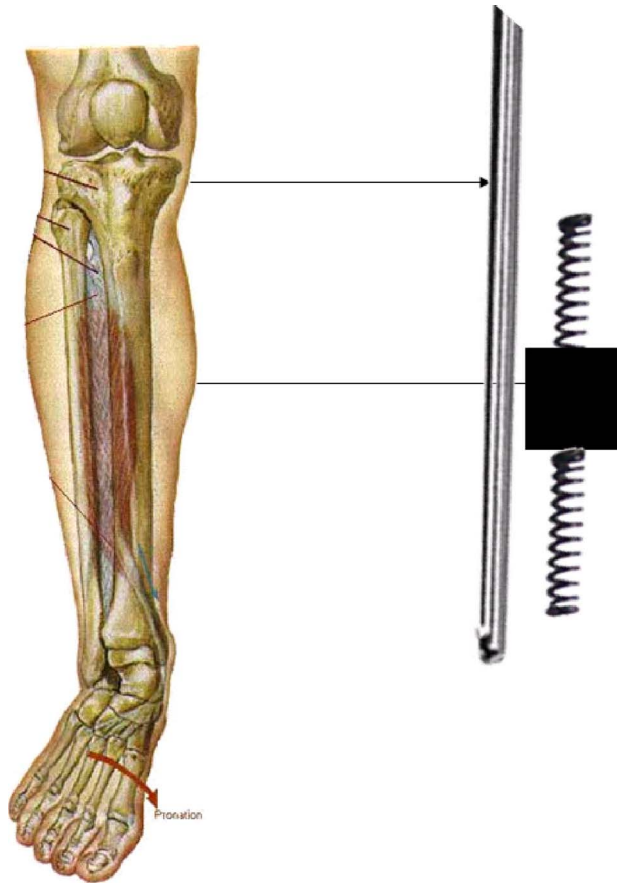

Fig. 11 The bone is represented by a rigid rod and the soft tissues are represented by a combination of springs and slider mass

periments when a subject will be asked to perform a simple planar motion with one segment, which will be fixed to an external device. Calculating the segment motion, using the presented methods, will be compared with a measured motion of the rigid external device.

Acknowledgment

M.S. would like to thank the Diane and Leonard Sherman Interdisciplinary Graduate School Fellowship and the Gutwirth Fellowship.

Appendix

Applying the PCT technique on the measurements of a rigid moving segment (measured using optic-electromotion system) causes two undesirable phenomena:

(1) In several cases, the rotation matrix extracted from the inertia tensor had a determinate of -1, which describes reflection instead of rotation.
(2) In several cases, the rotation matrix described the legal rotation matrix (determinant equals to 1) but compared with the rotation matrix in the previous time step, two axes were rotated by 180 deg, which is not a reasonable incremental deformation.

In order to correct the two undesirable phenomena, correction algorithms were introduced as follows.

The rotation matrix can be presented as three axes (vectors) as follows:

$$R(t_s) = [e(t_s)_1 \quad e(t_s)_2 \quad e(t_s)_3] \tag{A1}$$

The first phenomenon occurs when the cross product of two axes does not yield the third axis. Therefore, for each time step, after the optimization algorithm is applied and a rotation matrix was calculated, three inequalities were examined as follows:

$$(e_i \times e_j) - e_k < \varepsilon \tag{A2}$$

where $i \neq j \neq k$ have the values of 1, 2, and 3 for $i=1$, and are permuted cyclically for $i=2$ and $i=3$. ε is set to a small value (for this study it was chosen as $\varepsilon=0.001$). In false cases, the direction of the third axis was rotated by 180 deg by

$$e_k = -e_k \tag{A3}$$

The correction of the second phenomenon, where two axes rotated by 180 deg, compared with the previous position, was done by examination of the below inequalities:

$$e_{i-1} \cdot e_i < 0, \quad i = 1,2,3 \tag{A4}$$

In the case of a false sentence, the direction of the (i) axis was rotated by 180 deg (Eq. (A3)).

References

[1] Chan, M., 1993, *Evaluation of the Use of Knee Braces Based on the Intrinsic Kinematics of a Normal Knee*, MIT, Cambridge, MA.
[2] Lafortune, M. A., Cavanaugh, P. R., Sommer, H. J., and Kalenak, A., 1992, "Three-Dimensional Kinematics of the Human Knee During Walking," J. Biomech., **25**, pp. 347–357.
[3] Murphy, M. C., and Mann, R. W., 1991, "Estimation of the Instantaneous Kinematics of the Normal Human Knee In Vivo," 37th Annual Meeting of the Orthopaedic Research Society, Anaheim, CA.
[4] Andriacchi, T. P., Alexander, E. J., Toney, M. K., Dyrby, C., and Sum, J., 1998, "A Point Cluster Method for In Vivo Motion Analysis: Applied to a Study of Knee Kinematics," ASME J. Biomech. Eng., **120**, pp. 743–749.
[5] Manal, K., McClay, I., Galinat, B., and Stanhope, S., 2003, "The Accuracy of Estimating Proximal Tibial Translation During Natural Cadence Walking: One vs. Skin Mounted Targets," Clin. Biomech. (Bristol, Avon), **18**, pp. 126–131.
[6] Cappello, A., Stagni, R., Fantozzi, S., and Leardini, A., 2005, "Soft Tissue Artifact Compensation in Knee Kinematics by Double Anatomical Landmark Calibration: Performance of a Novel Method During Selected Motor Tasks," IEEE Trans. Biomed. Eng., **52**(6), pp. 992–998.
[7] Cerveri, P., Rabuffetti, M., Pedotti, V., and Ferrigno, G., 2003, "Real-Time Human Motion Estimation Using Biomechanical Models and Non-Linear State-Space Filters," Med. Biol. Eng. Comput., **41**, pp. 109–123.
[8] Reinschmidt, C., Van Den Bogert, A. J., Lundberg, A., Nigg, B. M., and Murphy, N., 1997, "Effect of Skin Movement on the Analysis of Skeletal Knee Joint Motion During Running," J. Biomech., **30**(7), pp. 729–732.
[9] Ryu, J. H., Kouchi, M., Mochimaru, M., and Lee, K. H., 2003, "Analysis of Skin Movements With Respect to Bone Motions Using MR Images," International Journal of CAD/CAM, **3**(2), pp. 61–66.
[10] Chèze, L., Fregly, B. J., and Dimnet, J., 1995, "A Solidification Procedure to Facilitate Kinematic Analysis Based on Video System Data," J. Biomech., **28**, pp. 879–884.
[11] Leardini, A., Chiari, L., Croce, U. D., and Cappozzo, A., 2005, "Human Movement Analysis Using Stereophotogrammetry—Part 3: Soft Tissue Artifact Assessment and Compensation," Gait and Posture, **21**, pp. 212–225.
[12] Vithani, A. R., and Gupta, K. C., 2004, "Estimation of Object Kinematics From Point Data," J. Mech. Des., **126**, pp. 16–21.
[13] Lu, T.-W., and O'Connor, J. J., 1999, "Bone Position Estimation From Skin Marker Co-Ordinates Using Global Optimisation With Joint Constraints," J. Biomech., **32**, pp. 129–134.
[14] Cerveri, P., Pedotti, A., and Ferrigno, G., 2004, "Non-Invasive Approach Towards the In Vivo Estimation of 3D Inter-Vertebral Movements: Methods and Preliminary Results," Med. Eng. Phys., **26**, pp. 841–853.
[15] Choset, H., Lynch, K. M., Hutchinson, S., Kantor, G., Burgard, W., Kavraki, L. E., and Thrun, S., 2005, "Kalman Filtering," *Principles of Robot Motion: Theory, Algorithms, and Implementation*, Massachusetts Institute of Technology, Cambridge, MA, pp. 269–301.
[16] Fioretti, S., and Jetto, L., 1989, "Accurate Derivative Estimation From Noisy Data: A State-Space Approach," Int. J. Syst. Sci., **20**(1), pp. 33–53.
[17] David, A. W., 1930, *Biomechanics and Motor Control of Human Movement*, Wiley, New York, pp. 33–45.
[18] Vicon Motion Systems and Peak Performance Inc., 2007, http://www.vicon.com.

Downloaded From: http://biomechanical.asmedigitalcollection.asme.org/ on 01/12/2015 Terms of Use: http://asme.org/terms